Modelling the potential of adsorbed hydrogen for use in aviation

Jessica E. Sharpe[a, b], Nuno Bimbo[b], Valeska P. Ting[b], Bruno Rechain[c], Emmanuel Joubert [c], Timothy J. Mays[b, *]

[a] *Doctoral Training Centre in Sustainable Chemical Technologies, University of Bath, Bath BA2 7AY, UK*

[b] *Department of Chemical Engineering, University of Bath, Bath BA2 7AY, UK*

[c] *Airbus Group Innovations, 92150 Suresnes, France*

*Corresponding author:

Room 3.02, 9W Building, Department of Chemical Engineering, University of Bath, Bath, BA2 7AY, United Kingdom.

phone: +44 (0) 1225 386 528

fax: +44 (0) 1225 385 710

email: T.J.Mays@bath.ac.uk

Abstract

A novel method for modelling the amount of hydrogen in high-pressure tanks containing varying quantities of adsorbent has been extended to allow calculation of the energy density and the specific energy of the storage system. An example calculation, using TE7 activated carbon beads as an adsorbent, has been conducted over a range of temperatures and compared to alternative energy storage methods, including conventional high-pressure methods. The results indicate that adsorption of hydrogen results in a higher energy density than direct compression up to a certain pressure, which is dependent on the temperature.

A preliminary comparison shows adsorbed hydrogen to be superior to battery storage technologies for both energy density and specific energy stored, although further calculations are required to expand the system boundaries used. Adsorbed hydrogen in a range of materials resulted in much lower energy density and specific energy than standard jet fuels such as kerosene, proving that advancement in the materials is required, especially intrinsic hydrogen storage capacity, before adsorption becomes a competitive energy storage technology for aviation.

Keywords

Hydrogen adsorption, porous solids, design curves.

Nomenclature

Symbol	Unit	Definition
V_C	cm^3	Container volume
V_B	cm^3	Bulk hydrogen volume
V_D	cm^3	Displaced volume
V_T	cm^3	Total adsorbate volume
V_F	cm^3	Volume of tank containing adsorbent
V_{BI}	cm^3	Volume of bulk hydrogen in the interstitial sites
V_{BC}	cm^3	Volume of bulk hydrogen in the tank containing no adsorbent
V_{BP}	cm^3	Volume of bulk hydrogen in the pores of the adsorbent
V_S	cm^3	Skeletal volume of the adsorbent
V_P	cm^3	Open pore volume
V_A	cm^3	Adsorbate volume
f	-	Fill factor
x	-	Packing factor of adsorbent
Θ_A	-	Fractional filling of the pore
v_P	$cm^3\ g^{-1}$	Pore volume per unit mass of adsorbent
m_S	g	Mass of the adsorbent
m_H	g	Mass of hydrogen
ρ_B	$g\ cm^{-3}$	Density of bulk hydrogen
ρ_A	$g\ cm^{-3}$	Density of adsorbate
ρ_S	$g\ cm^{-3}$	Skeletal density
E_H	MJ	Energy available
m_W	g	Mass of the system
m_S	g	Mass of the adsorbent
b	MPa^{-1}	Affinity parameter

c	-	Heterogeneity parameter
Z	-	Compressibility factor
P	MPa	Pressure
P_B	MPa	Breakeven pressure
M	g mol^{-1}	Molar mass
R	cm^3 MPa K^{-1} mol^{-1}	Gas constant
T	K	Temperature

1. Introduction

Hydrogen shows great potential as an energy store as it can be produced sustainably, it has the highest energy per unit mass of any chemical fuel, it is abundant in water and biomass, and only water is produced as a by-product when releasing the stored energy. However, hydrogen has a very low energy density per unit volume which is problematic when using it as an energy vector. To make hydrogen commercially viable the volumetric density (*i.e*. its mass per unit volume) needs to be vastly increased, particularly for applications where low mass and low volumes are required, such as in aviation. Physisorption of molecular hydrogen (H_2) in nanoporous materials is one promising method of doing this and may improve on conventional storage methods, such as liquid H_2 at low temperature (< 33 K) or high pressure gas (up to 70 MPa). Adsorptive storage is beneficial over chemisorption (storing hydrogen chemically bonded to other elements) in that it does not require large energy inputs to recover the stored hydrogen from the adsorbent, due to the relatively weak interaction between the adsorbent and hydrogen. However, because of these weak interactions, low temperatures are required in order to store large quantities of hydrogen.

Aviation is one industry within which emissions must be rapidly reduced. Using conventional jet fuel such as kerosene results in the production of 2-3 % of all global carbon emissions [1], as well as releasing short lived gases directly into the upper atmosphere, which results in an increase in the radiative forcing values of these gases and so causing large impacts on global warming [2-4].

Hydrogen has the potential to be a cleaner, safer fuel, whilst improving performance, lowering direct operating costs, and having a more favourable availability and economic impact compared to current jet fuels [5, 6]. There have been various hydrogen prototype planes such as the Tupolev Tu-155 [7], the Antares DLR-H2 [8], the Boeing phantom eye [9] and the ENFICA-FC Rapid 200-FC [10], all of which have

utilised the current conventional hydrogen storage methods of compression or liquefaction.

Physisorption of hydrogen has not been used in aircraft to date due to the immaturity of the technology. The potential issue with the use of physisorption of hydrogen over direct compression is the additional requirement of the adsorbent in the tank, as aircraft require very low weight technology [11].

In order for the benefits of adsorptive storage of hydrogen to be quantified, there is a need for a method for calculating the amount of energy stored *via* hydrogen per unit volume and per unit mass of the system. This equation has been derived, from which the comparison between compressed hydrogen and physisorbed hydrogen can be made, and additionally can be loosely compared to other potential aircraft propulsion systems including kerosene, lithium-ion batteries and lead-acid batteries.

2. Materials and Methods

All materials and methods used in this work are equivalent to that in our previous work [12].

3. Theory and calculation

3.1. The new model for a tank filled with an adsorbent

We have previously derived a method for comparing the amount of hydrogen stored in a set volume when using varying quantities of adsorbent, which can be depicted as a design curve [13]. These equations have been altered to account for a density variation within the pores of nanoporous materials, as described in our previous work [12], which we believe to be a more accurate representation of the hydrogen in the pores. The development of this model presented here includes a factor to account for the hydrogen in the intergranular space, as observed in Fig. 1, where V_C represents the volume of the container, V_B is the volume of the bulk hydrogen, V_D is the displaced

volume, V_T is the total volume of the adsorbent, and V_F is the volume of the tank containing the adsorbent (V_T plus intergranular volume). The bulk hydrogen contribution can be separated into the following volumes: V_{BI} is the volume of the bulk hydrogen in the interstitial sites between the adsorbent, V_{BC} is the volume of the bulk hydrogen in the section of the container containing no adsorbent and V_{BP} is the volume of the bulk hydrogen in the pores of the adsorbent. The skeletal volume of the adsorbent including the closed pores is V_S, the open pore volume is V_P, and the volume of the adsorbate is V_A. f is the fill factor indicating the ratio of the volume of the tank containing the adsorbent to the total volume of the tank, x is the packing factor of the adsorbent, indicating the ratio of the total volume of the adsorbent to the total volume of the adsorbent plus intergranular space, Θ_A is the fractional filling of the pore *i.e*. the ratio of the adsorbate volume to the pore volume, and v_P is the pore volume per unit mass of the adsorbent, m_S, after degassing.

Fig. 1 – Representation of the nomenclature used to calculate the amount of hydrogen in a tank containing adsorbent.

Using this nomenclature, the following derivation for the total amount of hydrogen within a tank containing adsorbent is achieved,

$$m_H = \rho_B V_B + \rho_A V_A \tag{1}$$

where m_H is the mass of hydrogen, ρ_B is the density of bulk hydrogen and ρ_A is the density of the adsorbate.

$$m_H = \rho_B V_{BC} + \rho_B V_{BI} + \rho_B V_{BP} + \rho_A V_A \tag{1a}$$

$$m_H = \rho_B (V_C - V_F) + \rho_B (V_F - V_T) + \rho_B (V_P - V_A) + \rho_A V_A \tag{1b}$$

$$m_H = \rho_B V_C (1 - f) + \rho_B (fV_C - xfV_C) + \rho_B (V_P - V_A) + \rho_A V_A \tag{1c}$$

$$m_H = \rho_B V_C (1 - fx) + \rho_B v_P m_S (1 - \Theta_A) + \rho_A v_P m_S \Theta_A \tag{1d}$$

where v_P is the specific pore volume. The mass of the adsorbent can be varied and so the following substitution is required

$$m_S = \rho_S V_S \tag{2}$$

where ρ_S is the skeletal density

$$m_S = \rho_S (V_T - V_P) \tag{2a}$$

$$m_S = \rho_S (V_T - v_P m_S) \tag{2b}$$

Rearranging Eq. (2b) gives

$$m_S = \frac{V_T \rho_S}{1 + v_P \rho_S} \tag{2c}$$

Substituting Eq. (2c) into Eq. (1d) gives

$$m_H = \rho_B V_C (1 - fx) + \rho_B v_P \frac{V_T \rho_S}{1 + v_P \rho_S} (1 - \Theta_A) + \rho_A v_P \frac{V_T \rho_S}{1 + v_P \rho_S} \Theta_A \tag{3}$$

$$m_H = \rho_B V_C (1 - fx) + \frac{v_P V_T \rho_S}{1 + v_P \rho_S} \left(\rho_B (1 - \Theta_A) + \rho_A \Theta_A \right) \tag{3a}$$

$$m_H = \rho_B V_C (1 - fx) + \frac{xf V_C v_P \rho_S}{1 + v_P \rho_S} \left(\rho_B (1 - \Theta_A) + \rho_A \Theta_A \right) \tag{3b}$$

3.2. Introducing the design curve per unit volume and per unit mass

Eq. (3b) gives the total amount of hydrogen in a tank of volume, V_C. This can be easily rearranged to give the volumetric hydrogen capacity

$$\frac{m_H}{V_C} = \rho_B (1 - fx) + \frac{xf v_P \rho_S}{1 + v_P \rho_S} \left(\rho_B (1 - \Theta_A) + \rho_A \Theta_A \right) \tag{4}$$

(Note, this only includes the internal volume of the tank, introducing a bias if comparing to other systems such as batteries which require no additional tank.)

Eq. (4) can be adjusted to calculate the energy available per unit volume instead of the quantity of hydrogen available per unit volume, providing an easier comparison with other systems such as batteries and kerosene. The energy is accounted as follows, assuming the production of $H_2O(g)$ and not $H_2O(l)$

$$\frac{\Delta H_f\left(\mathrm{H_2O(g)}\right)}{M(H_2)} = \frac{241.8\,\mathrm{kJ\ mol^{-1}}}{2.016\,\mathrm{g\ mol^{-1}}} = 120\,\mathrm{MJ\ kg^{-1}} \tag{5}$$

Therefore, a factor of 120 can be used in order to convert Eq. (4) from grams of hydrogen per cm^3 to mega joules of energy available, E_H, per L.

$$\frac{E_H}{V_C} = 120\left(\rho_B\left(1-fx\right) + \frac{xfv_P\rho_S}{1+v_P\rho_S}\left(\rho_B\left(1-\Theta_A\right)+\rho_A\Theta_A\right)\right) \tag{6}$$

Eq. (3b) can also be adjusted in order to look at the amount of hydrogen stored per unit mass of the container, using the internal walls of the tank as the system boundary.

The mass of the contents of the tank, m_W, is $m_W = m_H + m_S$ (7), where m_S is the mass of the adsorbent and m_H is the mass of the hydrogen. The mass of the hydrogen has been calculated (Eq. (3b)) and the mass of the adsorbent is given in Eq. (2c). Substituting these into Eq. (7) gives

$$m_W = \frac{xfV_C\rho_S}{1+v_P\rho_S} + \rho_B V_C(1-fx) + \frac{xfV_C v_P\rho_S}{1+v_P\rho_S}\left(\rho_B\left(1-\Theta_A\right)+\rho_A\Theta_A\right) \tag{7a}$$

$$m_W = \rho_B V_C\left(1-fx\right) + \frac{xfV_C\rho_S}{1+v_P\rho_S}\left(1+v_P\rho_B\left(1-\Theta_A\right)+v_P\rho_A\Theta_A\right) \tag{7b}$$

Eq. (7b) and Eq. (3b) can be used to observe the amount of hydrogen per unit mass of the system

$$\frac{m_H}{m_W} = \frac{\rho_B V_C (1 - fx) + \frac{xfV_C v_P \rho_S}{1 + v_P \rho_S}\left(\rho_B \left(1 - \Theta_A\right) + \rho_A \Theta_A\right)}{\rho_B V_C \left(1 - fx\right) + \frac{xfV_C \rho_S}{1 + v_P \rho_S}\left(1 + v_P \rho_B \left(1 - \Theta_A\right) + v_P \rho_A \Theta_A\right)} \quad (7c)$$

Eq. (7c) utilises internal tank walls as the system boundary for the weight and so can be used to compare physisorption of hydrogen to direct compression but will not account for the different weights of the tanks required for each system, which is relevant as there are different types of tanks rated for different pressures. This limitation of the system boundary also makes it difficult to compare to other systems such as batteries, which do not require heavy tanks.

As previously reported for the hydrogen per unit volume, Eq. (7c) can be adjusted to account for the amount of energy per unit mass as opposed to the amount of hydrogen per unit mass

$$\frac{E_H}{m_W} = 120\left(\frac{\rho_B V_C \left(1 - fx\right) + \frac{xfV_C v_P \rho_S}{1 + v_P \rho_S}\left(\rho_B \left(1 - \Theta_A\right) + \rho_A \Theta_A\right)}{\rho_B V_C \left(1 - fx\right) + \frac{xfV_C \rho_S}{1 + v_P \rho_S}\left(1 + v_P \rho_B \left(1 - \Theta_A\right) + v_P \rho_A \Theta_A\right)}\right) \quad (8)$$

4. Results

4.1. Adsorption vs. compression

The TE7 carbon beads were chosen as an example adsorbent due to their low cost, availability and use as a previous reference material [14]. The TE7 carbon bead isotherms were collected at temperatures of 89, 102, 120 and 150 K, and the Tóth isotherm equation was used for the fractional filling of the pore, Θ_A [15],

$\Theta_A = \frac{bP}{\left(1 + \left(bP\right)^C\right)^{1/C}}$, where *b* is an affinity parameter, *C* is a heterogeneity parameter, and both were estimated using a non-linear fit on the isotherms and allowing them to vary with temperature, as shown in our previous work [12, 13]. The adsorbed density,

ρ_A, was also estimated from the fitting but assumed to be constant with temperature, although it is known that supercritical adsorbates undergo thermal expansion except when near saturation. The bulk density, ρ_B, was set as $\rho_B = (PM)/(ZRT)$, where Z is a compressibility factor, for which a rational function approximation of the Leachman equation of state was used, P is the pressure, R is the gas constant, and T is the temperature. F and x are variables, and ρ_S and v_P were determined experimentally.

Fig. 2 shows the volumetric energy density and specific energy, equivalent to the gravimetric energy density, (in a tank of 30 L internal volume) for a variety of temperatures, pressures, and amount of adsorbate. Arbitrary values were chosen for f and x to give a broad range of quantities of adsorbate; from direct compression of hydrogen ($f = 0$) to a combination of adsorption and direct compression of hydrogen ($0 < f < 1$) to complete adsorption of hydrogen ($f = 1$).

Fig. 2 – The energy available per unit volume (the energy density) (left) and per unit mass (the specific energy) (right) in a tank filled with varying quantities of TE7 carbon beads at different temperatures and pressures. The insets show zoomed regions of the same data.

Fig. 2 shows that for the volumetric energy density, there is a pressure up until which adsorption is favoured over compression, and above which compression is favoured over adsorption, known as the breakeven pressure, P_B.

Fig. 3 – The breakeven pressures for TE7 carbon beads at varying temperatures.

As seen in Fig. 3, when observing the volumetric energy density for the TE7 carbon beads there is an optimum temperature at which adsorption is favoured up to a higher pressure than direct compression, independent of the amount of adsorbent present, also observed in our previous work [13].

When observing the specific energy in Fig. 2, compression is always favoured. However, the broader the system boundaries, the higher the pressure that adsorption would be favoured over compression.

These calculations have also been performed for four other materials; a high surface area activated carbon, AX-21, and three metal-organic frameworks; MIL-53, NOTT-101 and MIL-101, all of which have been used for analysis in our previous work [12]. The results of these calculations can be found in the Supplementary Data. When we compare the breakeven pressures found for the energy density of each material against temperature, we observe that there does not appear to be an obvious trend.

Fig. 4 – The breakeven pressures for a range of materials.

For AX-21, MIL-53 and NOTT-101, within the temperature range studied for these materials, there appears to be a fairly linear increase in breakeven pressure with temperature. MIL-101 and the TE7 carbon beads both deviate from this trend and show an optimum temperature for the breakeven pressure.

Fig. 2, Fig. 3 and Fig. 4 suggest that, provided enough energy per unit volume and per unit mass can be stored *via* adsorption below the breakeven pressures, then adsorption is favourable to compression, as it diminishes the energy penalty of the storage system by using conditions closer to ambient. However, if more energy is required to be stored than is possible *via* adsorption in a set tank volume, compression at higher pressures would be a more successful method.

4.2. Comparison to alternative aircraft energy systems

It is very important to note the boundaries that have been used in these systems as mentioned in Section 3.2. For both the energy density and specific energy, the internal surface of the tank has been used as the system boundary, due to the uncertainty in the rest of the system. However, limiting the system to the internal volume of the tank does have its drawbacks, specifically in that it limits the accuracy of the comparison to other systems.

A preliminary comparison between the energy density and specific energy *via* hydrogen storage and alternative energy technologies is shown for the TE7 carbon beads at 89 K.

Fig. 5 – A comparison of potential aviation energy technologies per unit volume (left) and per unit mass (right), compared to hydrogen storage in a tank containing varying quantities of TE7 carbon beads at 89 K. The insets show zoomed regions of the same data.

Fig. 5 shows that hydrogen adsorption in TE7 carbon beads at 89 K has a much lower energy density and specific energy than kerosene at all pressures calculated. Compressed hydrogen has a higher specific energy than kerosene, but a much lower energy density. At high pressures, adsorbed hydrogen shows a higher energy density and specific energy than both battery technologies, but a complete comparison would require accounting for the full storage system. The system boundaries are particularly significant when comparing to battery storage, as these require no additional tank, making the quantities for adsorbed and compressed systems overrepresented in both graphs shown in Fig. 5.

It is also worth noting that these calculations do not take into account the amount of recoverable hydrogen, which can be significantly smaller than the amount of stored hydrogen, although this value depends on the conditions (temperature and pressure) at which the hydrogen is extracted from the tank. This is yet another bias in the calculations as the same issue would not be as important for either compressed hydrogen, kerosene or batteries.

The same trends observed in Fig. 5 are further confirmed in Fig. 6, which depicts the comparison of the energy density and specific energy of various energy storage technologies. The change in energy density and specific energy when using the different adsorbents is fairly insignificant when comparing to other systems such as kerosene.

Fig. 6 – (Left) The energy density and specific energy of various energy storage technologies. [16-18]. (Right) zoomed in to various hydrogen adsorption materials at 20 MPa in a tank half filled with adsorbent.

5. Conclusion

An equation has been successfully derived to calculate the energy density and specific energy for the adsorption of hydrogen in a tank containing varying quantities of adsorbent at different temperatures and pressures. It has been observed that when using this equation to directly compare the adsorption and compression of hydrogen, the energy density of hydrogen stored *via* adsorption is always better than that of compression up to a certain pressure, which for the TE7 carbon beads at 150 K is approximately 21 MPa. Therefore, for applications where small quantities of stored energy are required, adsorption is preferable to compression as it can occur at pressures closer to ambient.

Compression and adsorption of hydrogen are both deemed comparable to battery technologies in terms of energy density and specific energy, but cannot yet compete with standard jet fuels such as kerosene. For hydrogen to be utilised in aviation, materials with a higher hydrogen capacity are required in order to make the energy system comparable to current systems.

Acknowledgements

JES thanks the UK Engineering and Physical Sciences Research Council (EPSRC) Centre for Doctoral Training in Sustainable Chemical Technologies at the University of Bath (EP/G03768X/1), and also to Dr Agata Godula-Jopek from the Airbus Group Innovation, Munich, Germany for financial support. NB, VPT and TJM thank the EPSRC for funding via three SUPERGEN hydrogen energy projects (EP/J016454/1, EP/K021109/1, and EP/L018365/1), VPT thanks the University of Bath for funding via an EPSRC Development Fund grant and a Prize Research Fellowship, and VPT and TJM thank the EPSRC for supporting the latter stages of this work via its Delivery

Fund. The authors thank Anne Dailly (Chemical Sciences and Materials Systems Laboratory, General Motors Global Research and Development, Warren, MI, U.S) for providing the NOTT-101 data, and MAST Carbon International, UK, for the TE7 activated carbon beads.

References

[1] S. Blakey, L. Rye, C.W. Wilson, Aviation gas turbine alternative fuels: A review, Proceedings of the Combustion Institute, 33 (2011) 2863-2885.

[2] Intergovernmental Panel on Climate Change, Aviation and the Global Atmosphere: A Special Report of IPCC Working Groups I and III in Collaboration with the Scientific Assessment Panel to the Montreal Protocol on Substances that Deplete the Ozone Layer, Cambridge University Press1999.

[3] D.S. Lee, D.W. Fahey, P.M. Forster, P.J. Newton, R.C.N. Wit, L.L. Lim, B. Owen, R. Sausen, Aviation and global climate change in the 21st century, Atmospheric Environment, 43 (2009) 3520-3537.

[4] D.S. Lee, G. Pitari, V. Grewe, K. Gierens, J.E. Penner, A. Petzold, M.J. Prather, U. Schumann, A. Bais, T. Berntsen, D. Iachetti, L.L. Lim, R. Sausen, Transport impacts on atmosphere and climate: Aviation, Atmospheric Environment, 44 (2010) 4678-4734.

[5] İ. Yilmaz, M. İlbaş, M. Taştan, C. Tarhan, Investigation of hydrogen usage in aviation industry, Energy Conversion and Management, 63 (2012) 63-69.

[6] G.D. Brewer, Hydrogen aircraft technology, CRC Press1991.

[7] Tupolev, Cryogenic Aircraft - Development of Cryogenic Fuel Aircraft [Online], 2009. Available: http://www.tupolev.ru/English/Show.asp?SectionID=82 [Accessed 12/12 2011].

[8] Fuel Cell Works, DLR motor glider Antares takes off in Hamburg – powered by a fuel cell [Online], Hamburg, 2009. Available: http://fuelcellsworks.com/news/2009/07/07/dlr-motor-glider-antares-takes-off-in-hamburg-%E2%80%93-powered-by-a-fuel-cell/ [Accessed 01/02/2012 2012].

[9] R. Jackson, C. Haddox, Phantom Eye High Altitude Long Endurance Aircraft Unveiled, Boeing [Online], Chicago, 2010. Available:

http://www.boeing.com/Features/2010/07/bds_feat_phantom_eye_07_12_10.html [Accessed 26/01 2010].

[10] European Commission, World Records for EU-Funded Fuel Cell Powered Aircraft [Online], 2011. Available: http://ec.europa.eu/research/transport/projects/items/world_records_for_eu_funded_fuel_cell_powered_aircraft_en.htm [Accessed 01/02/2012 2012].

[11] M. Kaufmann, D. Zenkert, P. Wennhage, Integrated cost/weight optimization of aircraft structures, Struct Multidisc Optim, 41 (2010) 325-334.

[12] J. Sharpe, V.P. Ting, N. Bimbo, A.D. Burrows, D. Jiang, T.J. Mays, Supercritical Hydrogen Adsorption in Nanostructured Solids with Hydrogen Density Variation in Pores, Adsorption, 19 (2012) 643-652.

[13] N. Bimbo, V.P. Ting, J.E. Sharpe, T.J. Mays, Analysis of optimal conditions for adsorptive hydrogen storage in microporous solids, Colloids and Surfaces A: Physicochemical and Engineering Aspects, 437 (2013) 113-119.

[14] A. Hruzewicz-Kołodziejczyk, V.P. Ting, N. Bimbo, T.J. Mays, Improving comparability of hydrogen storage capacities of nanoporous materials, Int. J. Hydrogen Energ., 37 (2012) 2728-2736.

[15] J. Toth, Gas-Dampf-Adsorption an festen Oberflächen inhomogener Aktivitäten, Acta Chim. Acad. Sci. Hung., 30 (1962).

[16] Y. Demirel, Energy: Production, Conversion, Storage, Conservation, and Coupling, Springer2012.

[17] S. Al-Hallaj, K. Kiszynski, Hybrid Hydrogen Systems: Stationary and Transportation Applications, Springer2011.

[18] D.Y. Goswami, F. Kreith, Energy Conversion, Taylor & Francis2007.

Figure captions

Fig. 1 – Representation of the nomenclature used to calculate the amount of hydrogen in a tank containing adsorbent.

Fig. 2 – The energy available per unit volume (the energy density) (left) and per unit mass (the specific energy) (right) in a tank filled with varying quantities of TE7 carbon beads at different temperatures and pressures. The insets show zoomed regions of the same data.

Fig. 3 – The breakeven pressures for TE7 carbon beads at varying temperatures.

Fig. 4 – The breakeven pressures for a range of materials.

Fig. 5 – A comparison of potential aviation energy technologies per unit volume (left) and per unit mass (right), compared to hydrogen storage in a tank containing varying quantities of TE7 carbon beads at 89 K. The insets show zoomed regions of the same data.

Fig. 6 – (Left) The energy density and specific energy of various energy storage technologies. (Right) zoomed in to various hydrogen adsorption materials at 20 MPa in a tank half filled with adsorbent.

Figures

Colour reproduction on the Web only for all images.

Figure 1:

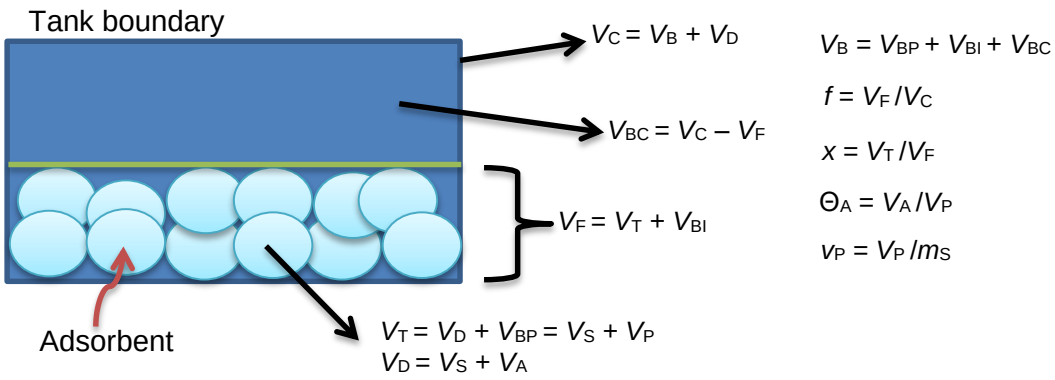
Tank boundary
$V_C = V_B + V_D$
$V_{BC} = V_C - V_F$
$V_F = V_T + V_{BI}$
Adsorbent
$V_T = V_D + V_{BP} = V_S + V_P$
$V_D = V_S + V_A$
$V_B = V_{BP} + V_{BI} + V_{BC}$
$f = V_F / V_C$
$x = V_T / V_F$
$\Theta_A = V_A / V_P$
$v_P = V_P / m_S$

Figure 2:

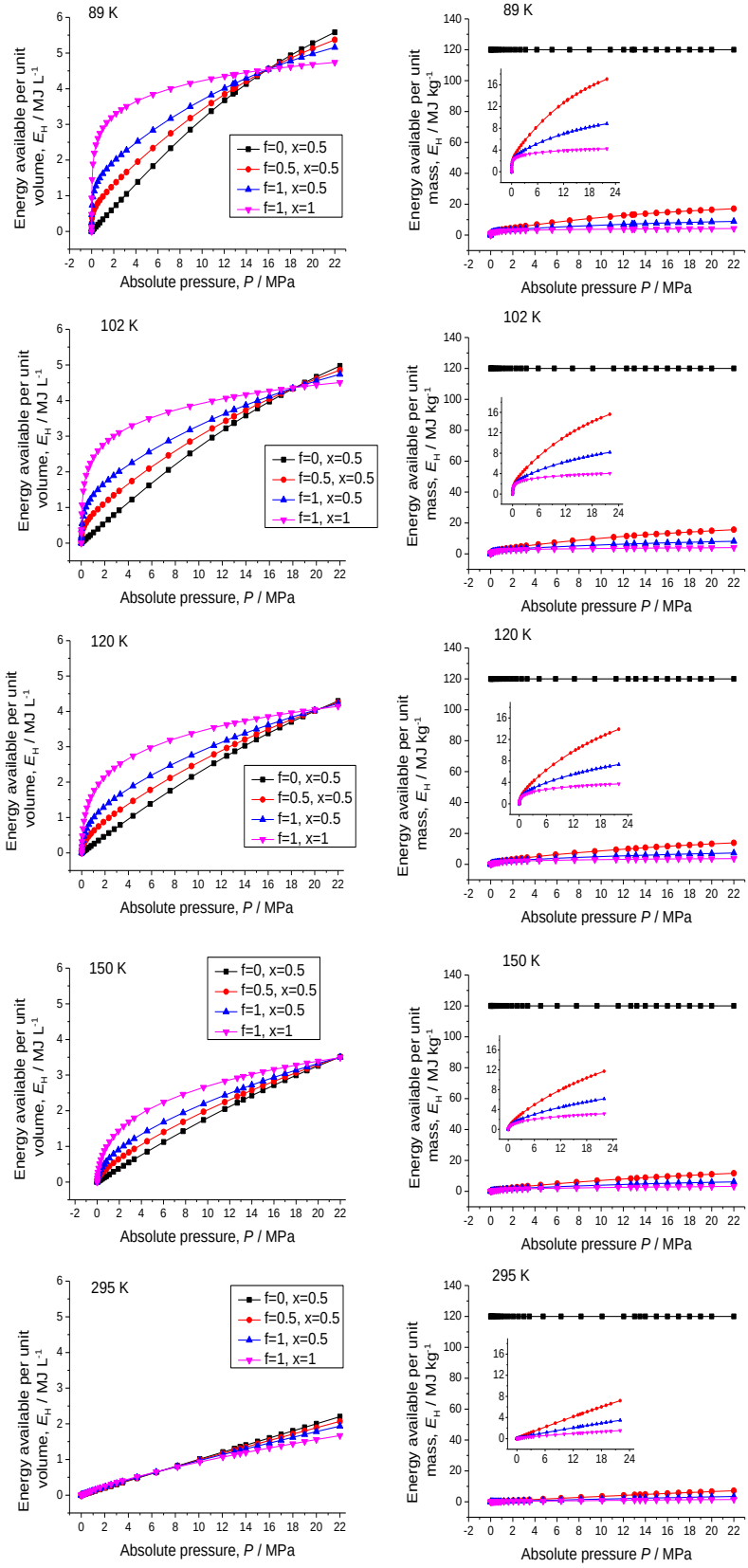
89 K
Energy available per unit volume, E_H / MJ L^{-1}
Absolute pressure, P / MPa
f=0, x=0.5
f=0.5, x=0.5
f=1, x=0.5
f=1, x=1
Energy available per unit mass, E_H / MJ kg^{-1}
Absolute pressure P / MPa
102 K
120 K
150 K
295 K

Figure 3:

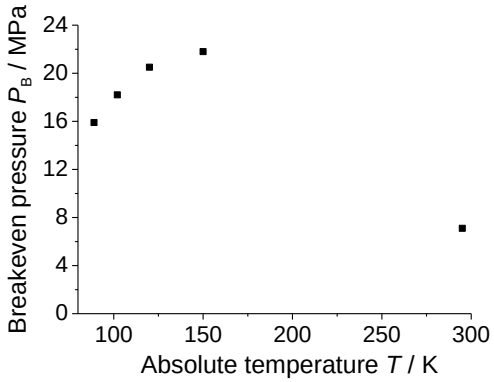

Figure 4:

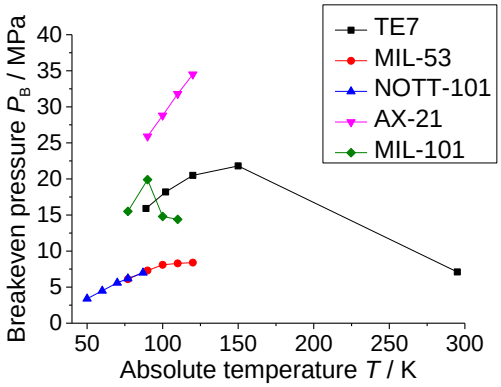

Figure 5:

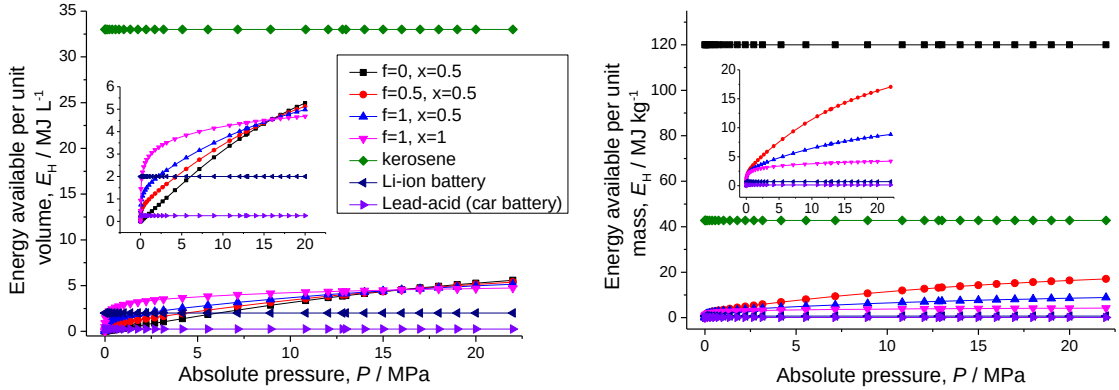

Figure 6:

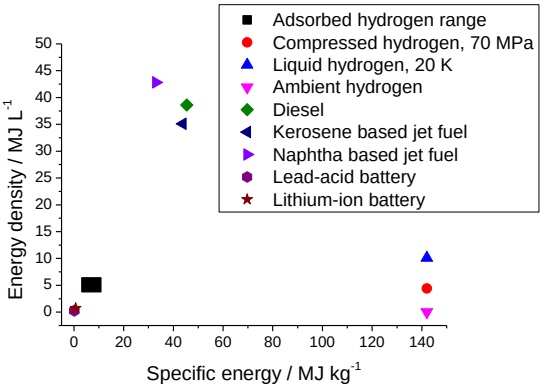
Adsorbed hydrogen range
Compressed hydrogen, 70 MPa
Liquid hydrogen, 20 K
Ambient hydrogen
Diesel
Kerosene based jet fuel
Naphtha based jet fuel
Lead-acid battery
Lithium-ion battery
Energy density / MJ L-1
Specific energy / MJ kg-1
0
5
10
15
20
25
30
35
40
45
50
0
20
40
60
80
100
120
140

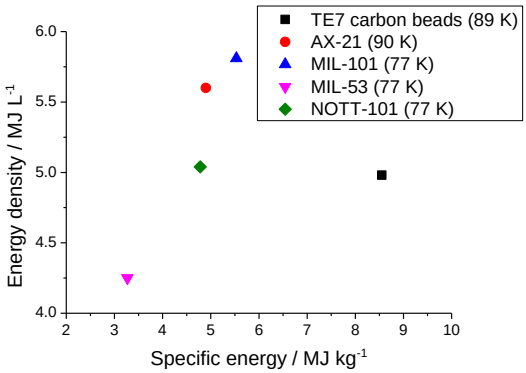
TE7 carbon beads (89 K)
AX-21 (90 K)
MIL-101 (77 K)
MIL-53 (77 K)
NOTT-101 (77 K)
Energy density / MJ L-1
Specific energy / MJ kg-1
4.0
4.5
5.0
5.5
6.0
2
3
4
5
6
7
8
9
10